Swelling dynamics of liquid crystal elastomers swollen with low molecular weight liquid crystals

Yusril Yusuf,* Yukitada Ono, and Yusuke Sumisaki
Department of Applied Quantum Physics and Nuclear Engineering, Graduate School of Engineering, Kyushu University, Fukuoka 812-8185, Japan

P. E. Cladis†
Advanced Liquid Crystal Technologies, P.O. Box 1314, Summit, New Jersey 07902, USA and Department of Applied Physics, Faculty of Engineering, Kyushu University, Fukuoka 812-8581, Japan

Helmut R. Brand
Theoretische Physik III, Universität Bayreuth, 95440 Bayreuth, Germany and Department of Applied Physics, Faculty of Engineering, Kyushu University, Fukuoka 812-8581, Japan

Heino Finkelmann
Makromolekulare Chemie, Universität Freiburg, 79104 Freiburg, Germany

Shoichi Kai‡
Department of Applied Quantum Physics and Nuclear Engineering, Graduate School of Engineering, Kyushu University, Fukuoka 812-8185, Japan; Department of Applied Physics, Faculty of Engineering, Kyushu University, Fukuoka 812-8581, Japan; and Graduate School of Systems Life Sciences, Kyushu University, Fukuoka 812-8581, Japan

(Received 28 July 2003; published 27 February 2004)

We experimentally investigated the swelling behavior of thin films ($\sim 150\ \mu$m) of liquid crystalline elastomers (LCEs) by low molecular weight liquid crystals (LMWLCs). The two LMWLCs used are the well-known nematic liquid crystals, 4-*n*-pentyl-4-cyanobiphenyl, and 4-methoxy-benzilidene-4-butyl-aniline. Both polydomain (POLY) and monodomain (MONO) LCE swelling are studied. In MONO LCEs (LSCEs), the director $\hat{\mathbf{n}}$ is uniformly oriented throughout the film. POLY films are made of many domains with different orientations. Its swelling behavior was similar to isotropic gels. In contrast, LSCEs revealed interesting results not anticipated by any theory. First, the LMWLC enters the LSCE by front propagation about three-times faster $\parallel\hat{\mathbf{n}}$ than $\perp\hat{\mathbf{n}}$. Second, only the LSCE dimensions $\perp\hat{\mathbf{n}}$ expanded, while that $\parallel\hat{\mathbf{n}}$ did not change at all. Third, when the LMWLC director and the LSCE director are aligned (MONO2 samples), swelling takes place about twice as fast as when they are not aligned. Volume change dynamics of swollen L(S)CEs investigated as a function of temperature revealed several phase transitions by optical and calorimetry techniques.

DOI: 10.1103/PhysRevE.69.021710 PACS number(s): 61.30.Gd, 83.80.Va, 05.70.Ln

I. INTRODUCTION

Liquid crystalline elastomers (LCEs) and gels are interesting because of their large mechanical response, for example, length changes as a function of temperature [1–3]. The LCE materials studied here were invented and developed by Finkelmann and co-workers [1–4]. The macroscopic behavior of these materials arises from the coupling between the elastic properties of the cross-linked siloxane polymer network and liquid crystalline degrees of freedom.

At first, only polydomain samples could be produced for which there are domains with different director orientations, denoted by a unit pseudovector **n** [1]. But then it was discovered that applying a large enough strain could reorient the domains giving rise to a uniform director orientation [2,4]. In 1991, Küpfer and Finkelmann [3] succeeded in generating monodomain samples, or liquid single crystal elastomers (LSCEs), by using two cross-linking steps with the second cross-linking step performed on a stretched film. These films turned out to have a spatially uniform **n** parallel to the stretching direction.

After the films have been cross linked, an external stress applied $\perp\hat{\mathbf{n}}$ can also lead to a reorientation of the director [5] observed as a stripe pattern on a length scale of several microns [6,7]. For directions $\parallel\hat{\mathbf{n}}$, no pattern formation is observed. All deformations are reversible as long as the films are not stretched beyond an elastic limit, typically two- or three-times threshold.

The structure of liquid crystalline elastomers, also referred to as LCEs in this paper, involves mesogenic groups chemically tethered as side chains to a cross-linked polymer network [1–4]. While LCEs exhibit a dramatic length and shape change at the nematic-isotropic phase transition, the cross-linked polymer network without side chains has no such phase transition. The dramatic length and shape change of LSCEs at the nematic-isotropic phase transition led to the

*Email address: yusuf@athena.ap.kyushu-u.ac.jp
†Email address: cladis@alct.com
‡Email address: kaitap@mbox.nc.kyushu-u.ac.jp

suggestion by de Gennes *et al*. that they may be useful components in artificial muscles [8,9].

Length changes as a function of temperature of LSCEs under variable external mechanical loads have been investigated in detail by Küpfer and Finkelmann [3,5]. In Ref. [10] piezo rheometry has been used to characterize the shear modulus as a function of frequency (in the low-frequency domain) and as a function of temperature for both, monodomain (MONO) and polydomain (POLY). In Ref. [4], it was found that LSCEs are ''beyond the critical point,'' meaning that there is no nematic-isotropic phase transition in LSCEs. In Ref. [11] this has been interpreted as being a consequence of ''frozen-in'' nematic order in LSCEs: even well above the apparent nematic-isotropic phase transition temperature, an LSCE film is still birefringent.

In Ref. [12], working with monodomain LCEs, it was found that there was a *spontaneous* shape change of LSCEs at nearly constant volume at the *apparent* nematic-isotropic liquid phase transition [12].

We underscore spontaneous because no external load had been applied to the material as was the case in previous work [3–5], and apparent because, in cross-linked LCEs, the nematic-isotropic phase transition ''disappears'' [11] above a critical cross-linking density.

The observations of thermally driven spontaneous shape changes in LSCE have been presented at various international conferences (for example, Ref. [12]). It was concluded that it gave ''proof of concept'' to the idea of LCEs as artificial muscles when cooperative orientation effects (i.e., the nematic-isotropic phase transition) of the side chains extended beyond a typical mesh size of the cross-linked polymer network. A similar conclusion was reached from investigations of polydomain samples under an external load [13].

The swelling of anisotropic LCEs in anisotropic solvents is a research topic that is only beginning to emerge [14]. Indeed, the only study other than ours we are aware of is the recent work of Uruyama *et al.* [15] who studied the equilibrium swelling of polydomain LCEs by LMWLCs. Here we present the results of our investigation of the swelling behavior of monodomain and polydomain LCEs swollen with the well-characterized LMWLCs, 4-*n*-pentyl-4-cyanobiphenyl (5CB), and 4-methoxy-benzilidene-4-butyl-aniline (MBBA). In addition to equilibrium aspects of swelling, we also study the time dependence for the different combinations of LCEs and LMWLCs available to us.

II. THE EXPERIMENT

A. LCE sample preparation

The LCE materials are prepared by polymer analog reaction of polymethyl-hydrogen-siloxane with an average degree of polymerization of about 60 and the monomeric mesogen 4-butenoxy-4-methyloxy benzoic acid phenylester ($CH_2{=}CH{-}CH_2{-}CH_2{-}O{-}$phenyl$-COO-$phenyl$-OCH_3$) and the cross-linking agent [$H_2{=}CH{-}O{-}(Si(CH_3)2{-}O)_{12}{-}CH{=}CH_2$]. The cross-linker agent is the oligomeric poly(dimethylsiloxane) with terminal vinyl groups. The concentration of the cross-linking (about 8%) is

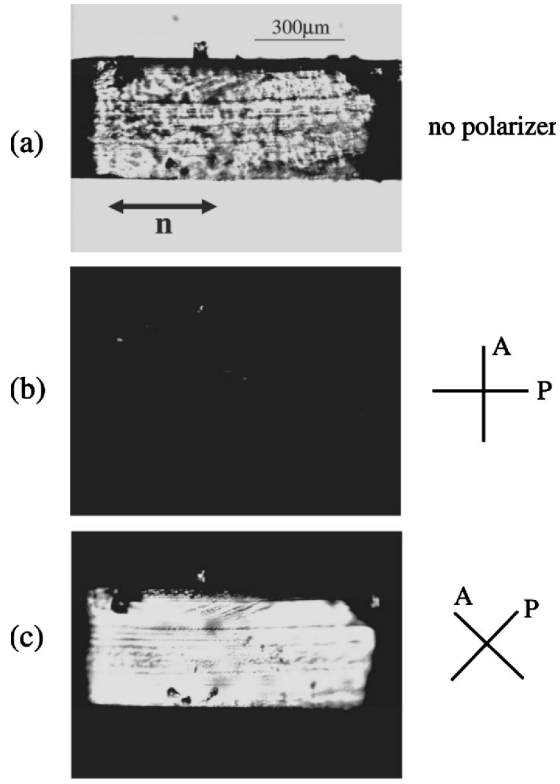

FIG. 1. Optical microscope pictures of dry MONO1 (planar): (a) no polarizers, (b) polarizers crossed parallel/perpendicular to $\hat{\mathbf{n}}$, shown below (a), and (c) polarizers rotated 45° to $\hat{\mathbf{n}}$. Sample thickness is $\sim 150\ \mu$m.

[3] related to the reactive vinyl groups. Except for the chemistry of the cross-linking agent, the procedure of the synthesis is described in Ref. [3].

The monodomain sample is obtained by mechanical stretching after gelation (after 3 h) to obtain the director orientation $\hat{\mathbf{n}}$ parallel to the stretching direction. The cross-linking reaction is completed with the sample stretched. This anisotropy was optically tested using crossed polarizers to confirm director orientation (Fig. 1).

While the lines $\|\hat{\mathbf{n}}$ in Figs. 1(a) and 1(c), are a typical feature of LSCEs, their origin is unknown. However, it has been known since 1991 [2] that there is a fairly strong tendency towards layering in side-chain monodomain LCEs, particularly when the cross linkers are rodlike [3]. Furthermore, in LCE monodomains, one clearly sees, even in the nematic phase, three orders of diffuse scattering that correlates with the molecular length of the side-chain LMWLCs. As a result, a tentative picture to emerge that may help put the swelling result described in the following sections into a context, is that the lines in Fig. 1 are grain boundaries between extended undulating monodomain regions generated in the tethered side-chain LMWLCs during stretching.

The siloxane backbone is dragged by the tethered side chains then locked in by the second cross-linking step into quasiregular ''pleated'' sheets that unfold easily $\perp\hat{\mathbf{n}}$ and not at all $\|\hat{\mathbf{n}}$.

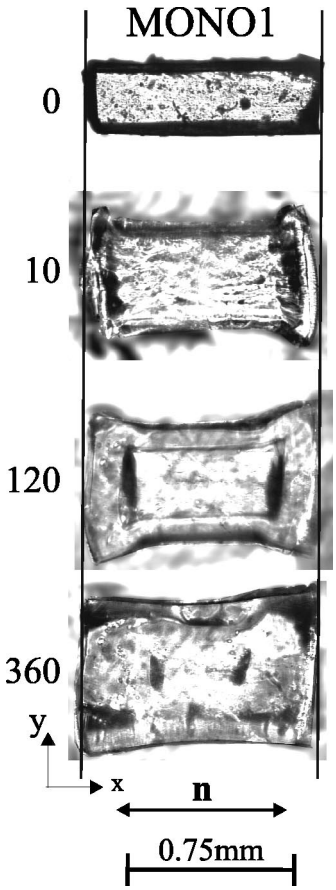

FIG. 2. MONO1, the numbers refer to minutes after the dry LCE was embedded in the LMWLC. In MONO1, the LMWLC reorients in a splay-bend front invading the LSCE along $\hat{x}$ and a twist front along $\hat{y}$. While MONO1 loses its rectangular shape at the initial stages of swelling, it recovers it at long times with a different aspect ratio. A remarkable feature is that the dimension of MONO1 parallel to $\hat{\mathbf{n}}$ does not change during swelling: LSCEs only swell $\perp \hat{\mathbf{n}}$.

B. Swelling sample preparation

To check the anisotropic swelling behavior of these samples, we prepared three types of rectangular LCE samples with different bulk director orientations $\hat{\mathbf{n}}$. One set of samples that we refer to as MONO1 is obtained by slicing parallel to $\hat{\mathbf{n}}$ (Fig. 2 top). A second set of samples MONO2 is obtained by slicing perpendicular to $\hat{\mathbf{n}}$ (Fig. 3). The third set of samples is obtained by slicing a polydomain film (Fig. 3). In other words, MONO1 is a planar aligned film, MONO2 is a homeotropically aligned film, and the POLY films have no alignment.

The films we prepare are ~ 150 μm thick and have an area of ~ 1.0 mm$\times 0.5$ mm. The samples are embedded in low molecular weight liquid crystals (anisotropic solvents) for swelling. In this study we use two nematic LMWLCs, 5CB and MBBA.

After slicing, LCE samples are embedded in the anisotropic solvent between two SiO coated glass plates. The thickness was controlled by a polymer (Mylar) spacer of 350 μm. The swelling behavior was observed in a polarizing microscope (Nikon) equipped with a hot stage (Mettler Toledo FP90 Central Processor) as temperature controller which can be simultaneously used for measurements of its thermal properties (heat capacity) via differential scanning calorimetry (DSC).

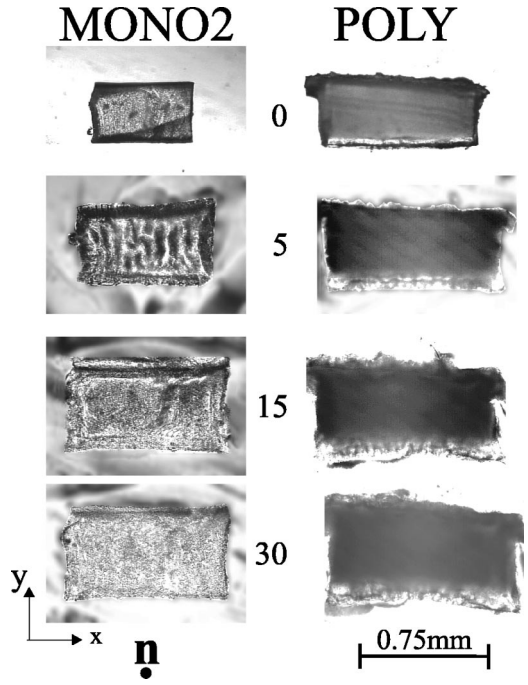

FIG. 3. MONO2 (left) and POLY (right) samples; the numbers refer to minutes after the dry LCE was embedded in the LMWLC. In the early stage of swelling, MONO2 conserves a rectangular profile (and aspect ratio) but buckles (stripe pattern) to conserve constant thickness as LMWLC floods into the LSCE faster than it can expand perpendicular to $\hat{\mathbf{n}}$. In MONO2, no director reorientation is required for the LMWLC as it invades the LSCE. POLY does not conserve its rectangular profile because domains where $\hat{\mathbf{n}}$ are perpendicular to the sample edges do not grow.

III. MEASUREMENTS AND DISCUSSIONS

A. Swelling dynamics

A qualitative sense of the shape changes during swelling of the samples is seen in Figs. 2 and 3. In the MONO1 samples, a rectangular front propagates in from the edges of the sample. We interpret this to be front propagation of the LMWLC into the LCE.

Figure 4 shows the linear reduction in the inside rectangle dimensions, F_x and F_y, as a function of time. From Fig. 4, we get $\dot{F}_x = 1$ μm/min and $\dot{F}_y = 0.33$ μm/min: this shows that the information about the orientation is transported about three-times faster $\perp \hat{\mathbf{n}}$ than it is $\| \hat{\mathbf{n}}$. Given that the sample dimension $\| \hat{\mathbf{n}}$ does not change, once inside the LSCE, the LMWLC moves three-times more easily $\perp \hat{\mathbf{n}}$ than it does $\| \hat{\mathbf{n}}$. Nevertheless, the LSCE sample dimension $\| \hat{\mathbf{n}}$ does not change during swelling at constant temperature.

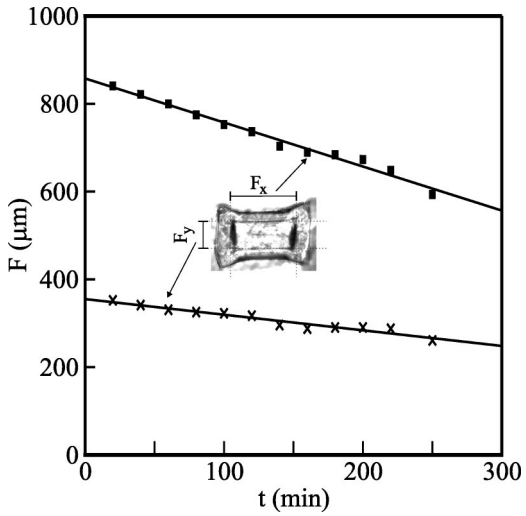

FIG. 4. Front propagation of LMWLC into the LCE. The inset shows the photomicrograph displayed in Fig. 2 after 120 min.

This difference in propagation speed can be interpreted as being due to the fact that nematic LCE monodomains show in their x-ray dffraction at small angles diffuse lines up to third order [3,16] indicating a certain degree of smectic layering.

We thus observe in our swelling experiments, the macroscopic evidence for strong smectic tendencies in LCE monodomains. The pronounced layering tendency locked into monodomain LCEs conserves the strong anisotropy of transport properties parallel and perpendicular to $\hat{\mathbf{n}}$ (Fig. 4). It also fixes the sample dimension parallel to $\hat{\mathbf{n}}$ because a shape change in this direction means that a whole new ''layer'' of LCE would have to be created (perhaps by the formation of energetic layer dislocations) as the LMWLC moves into the sample.

Front propagation occurs when a lower-energy state replaces a higher-energy state on macroscopic length scales (i.e., cooperatively) and, further, there is an interface separating the two states. The interpretation of the propagating rectangular interface, as LMWLCs invading the LSCE implies that the dry LCE is stressed and the low molecular weight LC relaxes these stresses leading to a net lower energy for the system.

In addition, in MONO1, but not in MONO2, the LMWLC reorients in the LCE stress field to be parallel to that of the LSCE frozen-in $\hat{\mathbf{n}}$ to minimize the orientational elastic energies of the LMWLC and the LSCE side chains. This implies that the LSCE side chains and the LMWLC form locally a binary mixture composed of untethered and tethered LMWLCs. In MONO2, the invading LMWLC has been prepared to have the same orientation as the LSCE so the reorientation step is not necessary and swelling takes place faster.

The director $\hat{\mathbf{n}}$ is defined by the orientation of the tethered LMWLCs [Fig. 5(a)]. In a monodomain, the mesogenic units are oriented parallel to the stretching direction [Fig. 5(b)]. The polymer backbones have very little order. In particular, they are not orientationally ordered on large length scales. However, as cross linking is done under stress in a nematic

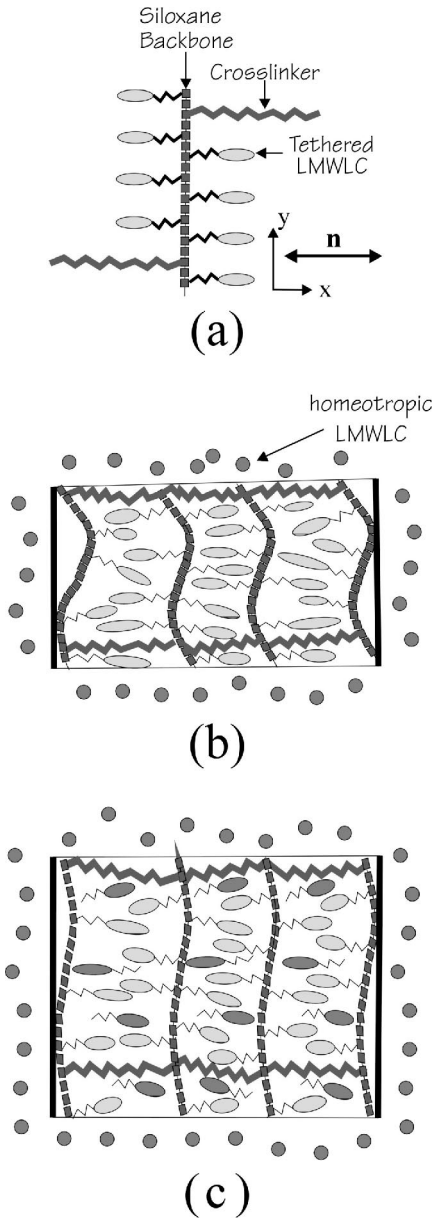

FIG. 5. Schematic picture of LSCE swelling process (a) LSCE ingredients. (b) LSCE embedded in homeotropic LMWLC. (c) LSCE swollen with LMWLC.

phase, the crosslinkers are no longer isotropically distributed and tend to extend in the direction of stretching. This gives rise to a tendency to fix a length scale $\|\hat{\mathbf{n}}$ in dry monodomains [Fig. 5(b)]. Of course, to make a three-dimensional (3D) network, there are also crosslinkers in the two direction perpendicular to the stretching direction [not shown in Fig. 5(b)].

This picture helps understand the swelling characteristics of LSCEs (e.g., Figs. 2 and 4). For example, to account for why the LSCE dimension parallel to the director does not change in the MONO geometry (Fig. 2), suppose in its dry state, the LSCE is in a strained configuration. During swelling, the LMWLCs can relax strains perpendicular to the director by preferential swelling samples in this direction (because it is much easier) without changing sample dimension

parallel $\hat{\mathbf{n}}$ (because it is more energetic). This leads to a structure with a length scale that is conserved during swelling. In a truly smectic phase, this is a consequence of conservation of layer numbers [Fig. 5(c)] i.e., new layers would have to be created to swell the monodomain parallel to $\hat{\mathbf{n}}$, which is a very energetic proposition.

In MONO1, the structure of the LMWLC front in Fig. 4 is such that far from the traveling interface $\hat{\mathbf{n}}\|\hat{z}$ and at the traveling interface $\hat{\mathbf{n}}\|\hat{x}$: the LMWLC front carries splay-bend deformation along $\hat{x}$ and twist deformation along $\hat{y}$. Splay-bend also has a back-flow transient that enhances the front speed while twist does not. A contributing factor to the conservation of the MONO1 length $\|\hat{\mathbf{n}}$ could be back-flow effects as the LMWLC invades the LSCE because its dimension $\|\hat{\mathbf{n}}\|\hat{x}$ has been fixed by the second cross-linking step.

We note again that in Fig. 2 the dimension of MONO1 parallel to $\hat{\mathbf{n}}$ does not change during swelling even though the LMWLC enters the LCE from the LCE surfaces perpendicular to $\hat{\mathbf{n}}$. Rather than expanding the LSCE in this direction ($\hat{x}$), the LMWLC spreads out in the $\hat{y}$ (also the $\hat{z}$) direction making these surfaces initially curved. Swelling proceeds from all edges to fill the sample up to two black ''holes'' ($t=360$ min in Fig. 2) that eventually disappear after about 10 h.

While this initial propagating phenomena can be clearly seen in the MONO1 sample because the orientation of the LMWLC propagating into the sample is $\perp$ to that of the LSCE (large difference in refractive indices), it is only observed in MONO2 in the first 20 min of swelling (Fig. 3) when the top and bottom surfaces buckle as LMWLC invades the LSCE faster than the swollen LSCE can stretch out to regain its flatness i.e., buckling instability to conserve constant thickness defined by the freezing in cross-linking step. Once the film is again flat (after about 5 min in Fig. 3), the buckling lines are gone.

It is also instructive to note that while the POLY sample does not retain its rectangular shape during swelling: regions where $\hat{\mathbf{n}}$ are perpendicular to a surface do not ''grow,'' its shape grows on average isotropically.

The picture to emerge is that there is a maximum volume of LMWLC that spontaneously invades the LCEs. We take $V(t)$ as the swelling elastomer volume at time t and $\Delta V = V - V_{max}$. There is an initial time regime where the LMWLC enters the LCE by front propagation and a long time regime where saturation is achieved as all the fronts merge and disappear inside the LCE.

To describe the volume changes we use an exponential growth process where $\Delta V/\Delta V_o = \exp(-t/\tau_s)$, where τ_s here is the relevant time constant. $\Delta V_o = V_o - V_{max}$ is the difference between the dry LCE volume (V_o) and the maximum swollen volume (V_{max}) or $\Delta V/\Delta V_o = \exp - t/\tau_s$.

Typically in what follows, we fit the volume (and length) changes to a simple exponential. The two parameters we obtain are the maximum swelling volume (from the maximum length changes) and the characteristic time scale for each geometry: MONO1, MONO2, and POLY and the two LMWLC swelling agents, 5CB, and MBBA. The length measurements are made far from elastomer corners and assume conservation of an orthogonal rectangular shape (but not its aspect ratio). Estimates of total volume changes under a particular set of conditions are deduced by multiplying the relevant length measurements.

B. Length expansion dynamics

To quantify these observations (Figs. 2 and 3), we define the length expansion parameter α_i for swelling as the ratio of the swollen length $\ell_i(t)$ to the initial dry length ℓ_i^0. Depending on the slicing direction, i may be x,y, or z. Length measurements were made in the middle of each edge far from other edges.

We underscore here (and have experimentally confirmed) that neither MONO1 nor MONO2 swell in the direction $\|\hat{\mathbf{n}}$. This is the $\hat{x}$ direction for MONO1 and the $\hat{z}$ direction for MONO2 in Fig. 6.

Figure 6 shows α_i for the three LCE geometries in the low molecular weight liquid crystal, 5CB. The time $t=0$ is the time of embedding the LCE in homeotropically oriented 5CB.

Figure 6(a) shows the swelling of MONO1. In the $\hat{y}$ direction (perpendicular to the director $\hat{\mathbf{n}}$), the relative length $\alpha_y = \ell_y/\ell_y^0$ increases exponentially in time (time constant $\tau_{M1} \sim 15.9$ min) and saturates at about 1.8 after $t=60$ min. In contrast, α_x is constant i.e., no length change is observed. The monodomain film cannot swell parallel to $\hat{\mathbf{n}}$ and $\hat{\mathbf{n}}$ of the LMWLC inside the LCE has reoriented from being $\|\hat{z}$ outside the elastomer to being parallel to the frozen-in director of the LSCE $\|\hat{x}$.

Figure 6(b) shows the length changes during swelling of MONO2. Both α_x and α_y increase exponentially in time and saturate with the maximum value about 1.8 ± 0.1. While the maximum length change $\perp \hat{\mathbf{n}}$ in MONO2 is the same as in MONO1, the time constant for swelling is $\tau_{M2} = 7.22$ min, about twice as fast as that of MONO1. This is because there is no reorientation process required of the LMWLCs' director to align with that of the LSCE, they are both $\|\hat{z}$. In MONO2, then, swelling in the plane $\perp \hat{\mathbf{n}}$ (the film plane) is isotropic, as expected.

Figures 6(a) and 6(b) show that length changes in monodomain LCE (LSCEs) by swelling with 5CB involves two steps: front propagation of LMWLC perpendicular to the LCE director (Figs. 2–4) and a reorientation process where the LMWLC director aligns with the LSCE director. When both share the same initial director orientation as they do in MONO2 [Fig. 6(b)], the characteristic time for swelling is nearly half that observed in MONO1 where the LMWLC director reorients as it propagates into the LCE [Fig. 6(a)].

Isotropic swelling in the film plane ($\perp \hat{z}$) is also observed for the polydomain LCE called POLY and shown in Fig. 6(c). Here both ℓ_x and ℓ_y increase exponentially in time ($\tau_P \sim 20.7$ min) and saturate at about $\alpha_{x,y}(t \to \infty) \sim 1.8 \pm 0.1$. But, in the POLY case (in contrast to MONO1 and MONO2), the dimension ℓ_z also expands in time, as do ℓ_x

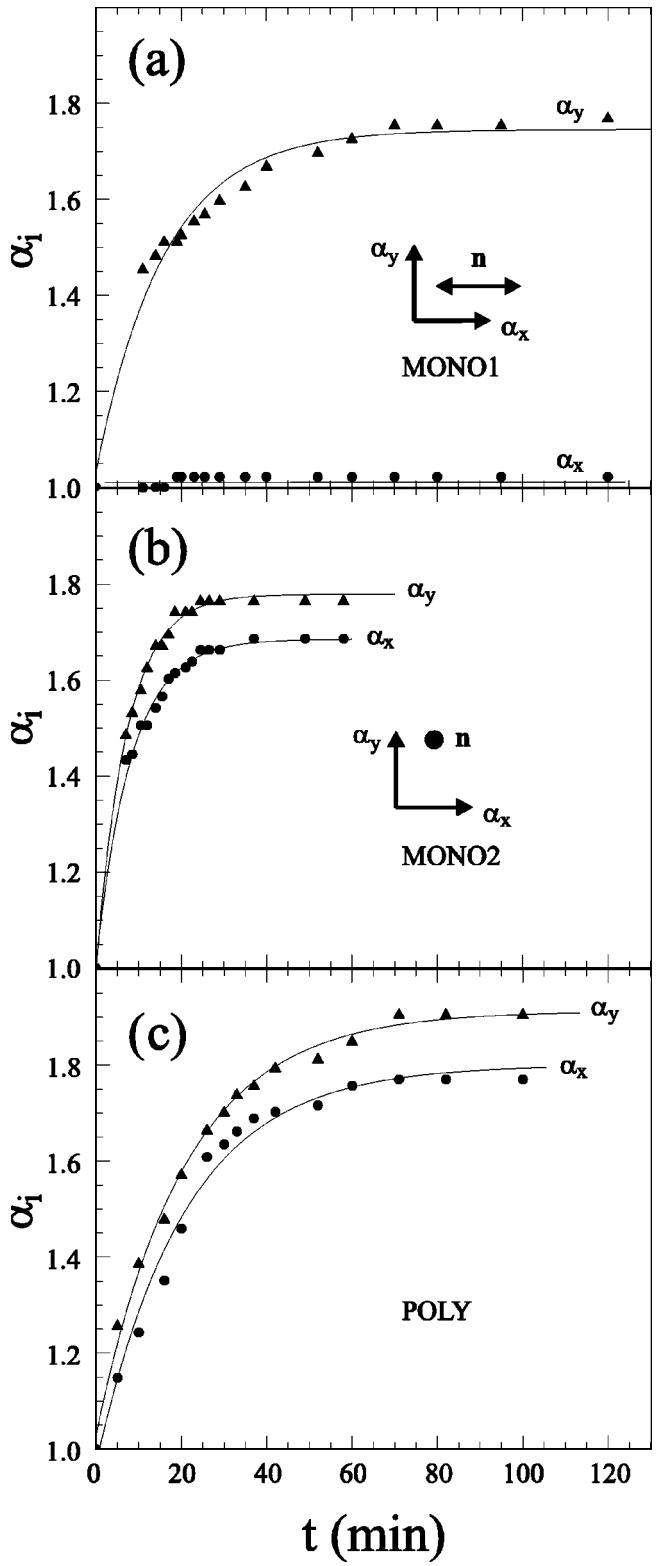

FIG. 6. Monodomain LCEs (LSCEs) only swell perpendicular to $\hat{\mathbf{n}}$ (a) and (b) and, on average, polydomain LCEs swell isotropically (c). When $\hat{\mathbf{n}}$ of the LMWLC is parallel to that of the LSCE (b), swelling saturates about twice as faster than as in (a) where it is perpendicular.

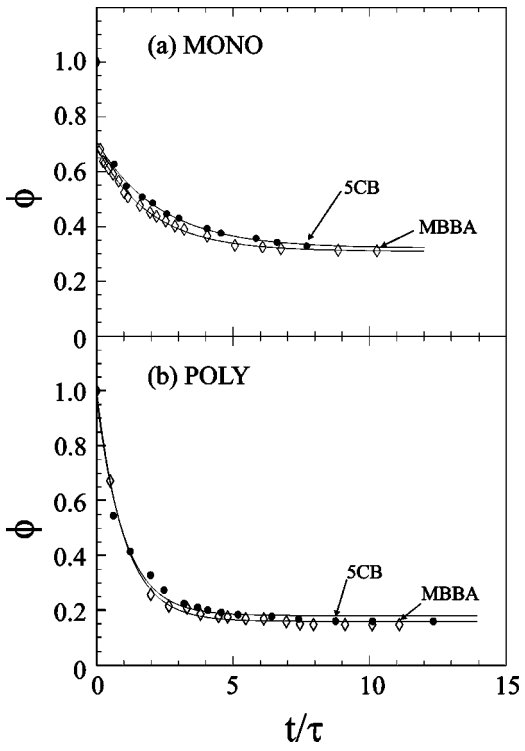

FIG. 7. Monodomain and polydomain inverse swelling volumes ϕ as a function of time t scaled by a relaxation time τ: ●5CB and ◇ MBBA. The solid lines in (a) are exponential fits to the data when the point at $t=0$, $\phi\equiv 1$ is excluded. We do this because the MONO (MONO1 in Fig. 2) measurements do not take into account relatively large shape changes of MONO1 in the vicinity of $t\sim 0$ (Fig. 2) as LMWLC propagates into the LSCE. In the case of POLY (b), a single exponential fit gives a reasonable fit when all points are included. The conclusion is that in POLY, there is only one time scale given by τ_P. In addition, POLY LCEs swell nearly twice as much as LSCEs [$\phi^P(t\to\infty)\sim 0.17$]. A POLY sample swells isotropically on average in 3D despite the fact that its surfaces become ragged on length scales comparable to the typical domain size.

and ℓ_y, at the same rate and with the same saturation, $\alpha_i(t\to\infty)\sim 1.8$, i.e., the same as $\alpha_{\perp\mathbf{n}}$ in MONO1 and MONO2. Polydomain LCEs swell isotropically as expected for an isotropic gel.

Similar behavior for all cases was observed when MBBA replaced 5CB.

C. Volume expansion time scales

Figure 7 shows universal plots for 5CB and MBBA of the volume fraction changes (ϕ) of monodomain and polydomain samples during the swelling process. ϕ was calculated as a whole from the average length changes of the swollen LCE and averaged mol fraction for all directions: $\phi=\ell_0^3/\ell(t)^3$. For POLY, this is just α_y^{-3}, [e.g., Fig. 6(c)]. As MONO is the MONO1 geometry in Figs. 2, 4, and 6, this is α_y^{-2} as $\alpha_x=1$ for MONO1 [Fig. 6(a)]. We define $\phi\equiv 1$ at time $t=0$. The volume fraction of the dry LCE is ϕ_o.

The relaxation times τ used to make Fig. 7 are obtained from fitting a time plot of ϕ to a single exponential. Including all the points in the fit, we get $\tau_{M1}^{5CB}=15.57$ min for

MONO1/5CB and $\tau_{M1}^{MBBA}=29.58$ min for MONO1/MBBA. For POLY/5CB, $\tau_P^{5CB}=8.10$ min and for POLY/MBBA, $\tau_P^{MBBA}=6.04$ min. In summary, the data show that the ''bare'' relaxation times are much longer for diffusion of LMWLCs into MONO1 than they are for POLY. And if we exclude the $t=0$ point for MONO1, they are even longer as we discuss as follows.

Exponential fits of Fig. 7, $\phi=\phi_\infty+\delta\phi_o\exp(-t/\xi\tau)$, show that a factor of 2 difference results depending on whether or not the first point at $t=0$ and $\phi=1$ is included in the fit for MONO1. When the point at $t=0$ and $\phi=1$ is not included [Fig. 7(a) solid gray lines], $\xi_{5CB}^M=2.31\pm0.19$, and $\xi_{MBBA}^M=1.96\pm0.08$: the time constants are about twice longer (and the fit is better) than when the first point is included for the MONO1 fit.

In contrast, the quality of the POLY exponential fits are not much changed when the $t=0$, $\phi\equiv1$ point is included in the fit.

The conclusion is that swelling MONO1 with LMWLC involves both diffusion of LMWLCs into LSCEs and reorientation: the LMWLC travels into MONO1 by front propagation then exponential relaxation takes place as the LMWLC reorients to align with the LSCE director. To quantify this conclusion, one must make 2D measurements of the LSCE shape during swelling.

D. Swollen vs dry LCE temperature response

Figure 8 shows dramatic differences in behavior between swollen LCEs and dry LCEs as a function of temperature. The typical length changes parallel and perpendicular to $\hat{\mathbf{n}}$ are shown in Figs. 8(a) and 8(b), respectively.

Increasing temperature at ~0.7 K/min, as expected, a dry LSCE monotonically shrinks parallel to $\hat{\mathbf{n}}$ (the $\hat{x}$ direction in Fig. 8) with a somewhat faster decrease in the vicinity of $T_c=82°$ C, the apparent nematic-isotropic phase transition temperature of the dry LSCE. It reaches its maximum shrinkage of about 72% just above T_c.

In directions perpendicular to $\hat{\mathbf{n}}$ [$\hat{y}$ Fig. 8(b)], the LSCE monotonically expands when heated to a maximum expansion corresponding to 123% just above T_c. The dry LSCE length changes are most dramatic in the vicinity of T_c.

In Fig. 9(a), the temperature dependence of volume, $\mathcal{V}(T)=\alpha_x\alpha_y^2\mathcal{V}_o$, of a dry LSCE is shown. With increasing temperature, the volume of dry LSCE slightly increases almost linearly up to 80 °C with about a $\sim1\%$ decrease at T_c. Above T_c, about a 6% volume expansion occurs when the tethered LMWLC side chains become isotropic at the LCE apparent nematic-isotropic transition and then saturates at about 1.08. Figure 9(a) shows that the nematic-isotropic phase transition of the dry LSCE is accompanied by a net volume increase. While length changes are large, the net volume change between room temperature and ~100 °C of the LSCE is only about 9% [Fig. 9(a)].

In the swollen LSCEs, relatively small length variations are observed predominantly around T_{NI} of the LMWLC ($T_{NI}\sim34.5$ °C for 5CB) and no remarkable changes at T_c (Fig. 8). A sharp ($\sim3\%$) decrease in length is observed in

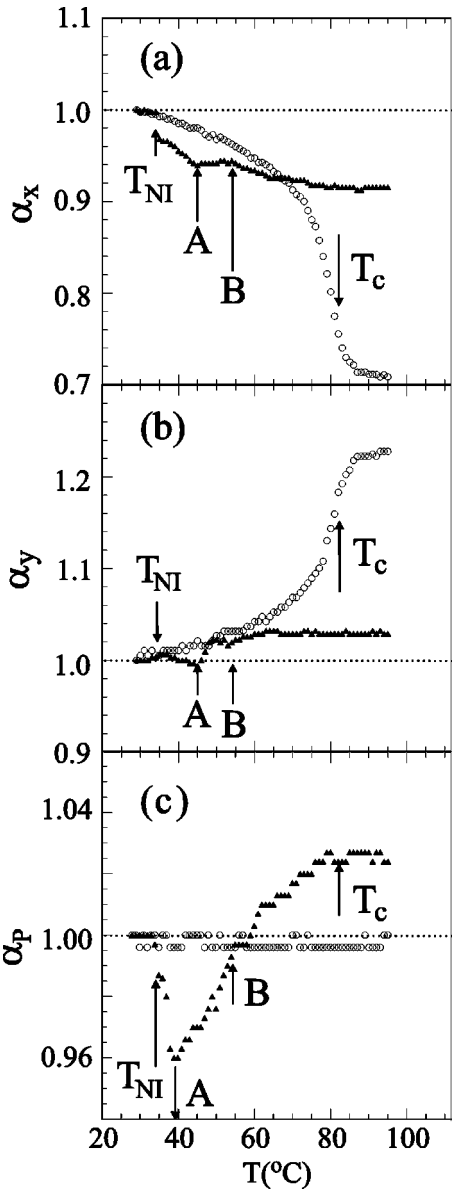

FIG. 8. Temperature dependence of relative length changes, α, during swelling for dry ○ and swollen LSCEs: ▲. (a) $\alpha_x\|\hat{\mathbf{n}}$, (b) $\alpha_y\perp\hat{\mathbf{n}}$ (also $\alpha_z\perp\hat{\mathbf{n}}$) for MONO1 [For MONO2, α_x in MONO1 should be replaced by α_z and α_y by α_x $(=\alpha_y)$.], and (c) POLY.

the LSCE length $\|\hat{\mathbf{n}}$ $(\hat{x})$ at T_{NI} and a slight increase is observed $\perp\hat{\mathbf{n}}$ $(\hat{y})$: a ''good'' LMWLC solvent above T_{NI} becomes ''bad'' parallel $\hat{\mathbf{n}}$ but remains relatively good at all temperatures $T>T_A$.

Here we use good in the sense that no local separation between the LMWLC and the tethered LC takes place, while for bad it does.

The effect of isotropic LMWLC solute (''guests'') is to shrink the network solvent (''hosts'') $\|\hat{\mathbf{n}}$ and expand it slightly $\perp\hat{\mathbf{n}}$ [Figs. 8(a) and 8(b)].

Figures 8(a) and 8(b) show a net volume decrease of $\sim2\%$ at T_{NI}: $\mathcal{V}(T)/\mathcal{V}_o=\alpha_x\alpha_y^2$ [Fig. 9(a)]. This is opposite to bulk LMWLCs where the jump at T_{NI} corresponds to a vol-

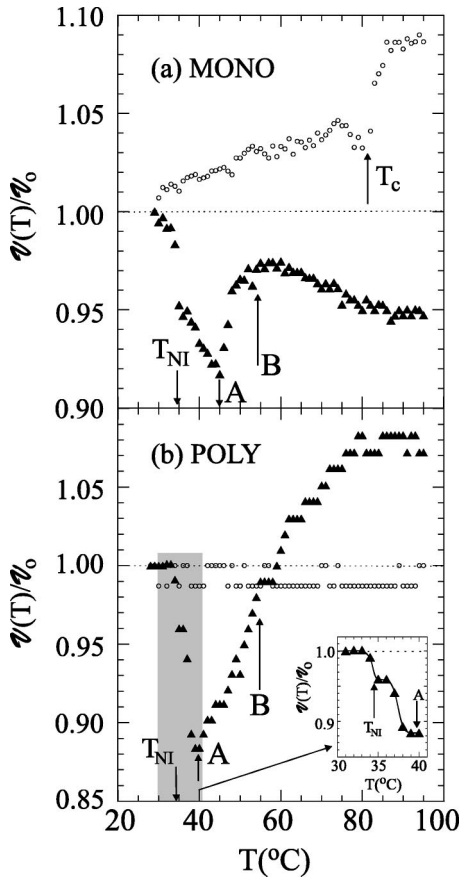

FIG. 9. Volume changes for MONO (a) and POLY (b) swollen ▲ and dry ○ LCEs. The inset graph shows details of the swelling data (shaded) in the vicinity of T_{NI}.

ume *increase* [17]. Between T_{NI} and T_A, the volume sharply decreases an additional ~ 5–6%, then rises back to its volume just below T_{NI}. For $T > T_B$, the volume decreases slightly to saturate above T_c at about $\sim 97\%$ $\mathcal{V}_o$.

The conclusion is that above T_{NI}, $\sim 2\%$ LMWLC is pushed out of the LSCE parallel $\hat{\mathbf{n}}$ [Fig. 8(a)]. Even more LMWLC is ejected between T_{NI} and T_A. Between T_{NI} and T_A, all lengths decrease with increasing temperature. The suggestion is that it is in this temperature range the LMWLC induces a nematic-isotropic phase transition in the LCE host which is completed at T_A. Once both guests and host are isotropic, LMWLC reenters the LSCE: the solvent loses its badness $\|\hat{\mathbf{n}}$ because there is no more $\hat{\mathbf{n}}$. But it always is relatively good $\perp \mathbf{n}$ [Fig. 8(b)]. Above $T > T_B$, while α_y is constant and greater than 1, α_x only weakly decreases with increasing temperature (Fig. 8).

According to the DSC measurements performed simultaneously for swollen LSCEs, a sharp peak is observed at T_{NI} and two broad small bumps are observed at T_A and T_B. This could be evidence of an *NI* transition taking place in the host LCE at T_A then remixing and in-take of more guest LMWLCs between T_A and T_B when both guests and host are isotropic to reach an equilibrium guest-host balance.

Further investigations, including 2D measurements of swollen L(S)CEs as a function of temperature are needed for more quantitative conclusions.

It is known that isotropic gels show no volume change with increasing temperature [18]. This is also the case for dry polydomain samples [Fig. 9(b)]: polydomain LCEs behave like isotropic elastomers. This seems reasonable as the orientational order of the side chains in polydomain LCEs is limited to small domains.

In contrast, a $\sim 4\%$ volume reduction occurs in swollen polydomains [Fig. 9(b)] at T_{NI} (5CB). This is about twice the reduction observed at T_{NI} in swollen LSCEs [Fig. 9(a)] where there is a uniform $\hat{\mathbf{n}}$ and the LMWLC solvent is only bad for lengths $\|\hat{\mathbf{n}}$ when $T > T_{NI}$ [Fig. 8(a)]. Presumably once the system as a whole becomes isotropic at T_A, the LMWLC solvent becomes good again and the swollen polydomain volume steadily increases to saturate at $\sim 107\%$ its room temperature volume just above T_c.

In POLY, T_{NI} and T_A are lower than their LSCE counterparts. In Fig. 9(b), $T_{NI} = 34.5\,^{\circ}\mathrm{C}$ and $T_A = 39.6\,^{\circ}\mathrm{C}$ compared to $T_{NI} = 34.7\,^{\circ}\mathrm{C}$ and $T_A = 45\,^{\circ}\mathrm{C}$ in MONO [Fig. 9(a)]. This is consistent with a greater reduction in transition temperatures with increased concentration of ''impurities,'' which in this case would be the guest LMWLC.

IV. SUMMARY AND PERSPECTIVES

We studied the swelling of LCEs with LMWLCs and found many surprising results not anticipated by any theory. We have interpreted some of our results using a liquid crystal guest-host perspective, where the guests are the LMWLCs and the host is the LCE. We have argued that this is a reasonable first step as LCEs are 92% mesogenic and only about 8% nonmesogenic, so liquid crystalline features can be expected to dominate when swelling L(S)CEs with LMWLCs.

(1) LSCEs that have been prepared using a stretching process do not swell in directions $\|\hat{\mathbf{n}}$. This is a remarkable result not anticipated by any theory. We suggest this is because the mesogenic cross linkers in the LCE system studied here tend to orient parallel to the tethered mesogenic side chains resulting in a network with quasismectic ordering, i.e., one with a large but fixed number of layers. Consequently, a swollen LCE cannot expand $\|\hat{\mathbf{n}}$ without a mechanism (such as dislocation motion) to generate complete layers.

(2) LSCE swelling is initiated by front propagation and a large shape change. Neither of these features has been anticipated by theory. We suggest that both these features are also related to the quasismectic structure laid down during the final cross-linking step of the LSCE.

(3) An intriguing undulation instablity is observed in homeotropic LSCEs when LMWLC propagates isotropically in 2D $\perp \hat{\mathbf{n}}$. The hypothesis is that this is a buckling transient to conserve the LCE dimension $\|\hat{\mathbf{n}}$. Once the sample flattens, the pattern disappears. Work is in progress to check this hypothesis.

(4) Polydomain LCEs swell isotropically in 3D, while LSCEs swell isotropically only in 2D and not at all in the third dimension. Thus, more LMWLCs (about 1.8 times more) enter polydomain LCEs than LSCEs. As the network

in both cases is chemically the same, we need to understand better the enhanced hospitality that grain boundary and dislocation dynamics of a quasilayered polydomain structure provides guest LMWLCs.

(5) For the temperature dependence of the swollen L(S)CEs, we have interpreted the volume jumps observed at T_{NI} (the nematic-isotropic transition temperature of the LMWLCs), T_A and T_B in a guest-host scenario. When the guests are isotropic but the host is nematic (T_{NI}), LMWLC is ejected from the host L(S)CE. When both guests and host are isotropic (T_A), the previously expelled guests reenter the host L(S)CE. At T_B, the host has reached its equilibrium shape in the nematic state (just below T_{NI}) and does not expand (in fact it shrinks with increasing temperature) more in LSCEs. On the other hand, in polydomain LCEs, the network keeps on expanding for $T>T_B$ up to saturation at $T \rightarrow T_c$, the dry LCE nematic-isotropic transition temperature. This last feature points to the importance of grain boundary and dislocation dynamics of a quasilayered polydomain structure that facilitates LCE swelling.

ACKNOWLEDGMENTS

We thank Nicole Aβfalg for sending us some of the samples. P.E.C. acknowledges the Japan Society for the Promotion of Science. This work was partially supported by the Japan-Germany Scientific Cooperative Program of Japan Society for the Promotion of Science and the Deutsche Forschungsgemeinschaft, and the Grant for Scientific Research sponsored by the Japan Society for the Promotion of Science. H.R.B. acknowledges the Deutsche Forschungsgemeinschaft for partial support of his work through Sonderforschungsbereich 481 Komplex Polymer und Hybridmaterialien in inneren und äußeren Feldern.

[1] H. Finkelmann, H.-J. Kock, and G. Rehage, Makromol. Chem., Rapid Commun. **2**, 317 (1981).

[2] An overview of research in liquid crystalline elastomers with a complete set of references up to 1997 is: H. R. Brand and H. Finkelmann, in *Physical Properties of Liquid Crystalline Elastomers*, edited by D. Demus *et al.*, Handbook of Liquid Crystals Vol. 3: High Molecular Weight Liquid Crystals (Wiley-VCH, Weinheim, 1998, p. 277.

[3] J. Küpfer and H. Finkelmann, Makromol. Chem. Rapid Commun. **12**, 717 (1991).

[4] S. Disch, C. Schmidt, and H. Finkelmann, Makromol. Chem. Rapid Commun. **15**, 303 (1994); S. Disch, C. Schmidt, and H. Finkelmann, *Liquid Single Crystal Elastomers, Polymeric Materials Encyclopedia* (CRC Press, Boca Raton, 1996).

[5] J. Küpfer and H. Finkelmann, Macromol. Chem. Phys. **195**, 1353 (1994).

[6] I. Kundler and H. Finkelmann, Makromol. Chem. Rapid Commun. **16**, 679 (1995).

[7] J. Weilepp and H.R. Brand, Europhys. Lett. **34**, 494 (1996), and references therein.

[8] P.G. de Gennes, M. Hubert, and R. Kant, Macromol. Symp. **113**, 39 (1997).

[9] M. Hubert, R. Kant, and P.G. de Gennes, J. Phys. I **7**, 909 (1997).

[10] P. Stein, N. Assfalg, H. Finkelmann, and P. Martinoty, Eur. Phys. J. E **4**, 255 (2001).

[11] H.R. Brand and K. Kawasaki, Makromol. Chem. Rapid Commun. **15**, 251 (1994); The nematic-isotropic phase transition is one of broken continuous symmetry. Therefore, a ''critical point'' leading to the disappearance of this phase transition is physically different from the gas-liquid critical point. See, e.g., P. E. Cladis, *Reentrant Phase Transitions in Liquid Crystals in Physical Properties of Liquid Crystals*, edited by D. Demus, J. Goodby, G. W. Gray, H.-W. Spiess, and V. Vill (Wiley-VCH, Weinheim, 1999), p. 289.

[12] P. E. Cladis, in *Phase Transitions in Liquid Crystalline Elastomers: A Fundamental Aspect of LCEs as Artificial Muscles*, edited by P. Erhard, D. H. Riley, and P. H. Steen, Interactive Dynamics of Convection and Solidification (Kluwer Academic Publishers, Dordrecht, 2001), p. 123.

[13] D.L. Thomsen III, P. Keller, J. Naciri, R. Pink, H. Jeon, D. Shenoy, and B.R. Ratna, Macromolecules **34**, 5868 (2001).

[14] Y. Yusuf, Y. Ono, Y. Sumisaki, and S. Kai, RIMS Report No. 1305, 2003, p. 139 (unpublished); Y. Ono, Master thesis Kyushu University, 2003.

[15] K. Uruyama, Y. Okuno, T. Nakao, and S. Kohjiya, J. Chem. Phys. **118**, 2903 (2003).

[16] I. Kundler and H. Finkelmann, Macromol. Chem. Phys. **199**, 677 (1998).

[17] F.R. Bouchet and P.E. Cladis, Mol. Cryst. Liq. Cryst. Lett. **64**, 81 (1980).

[18] See, for example, M. Doi, *Introduction to Polymer Physics* (Oxford University Press, Oxford, 1997), p. 63.